Electronic Supplementary Material (ESI) for Physical Chemistry Chemical Physics.

# Probing the Charge Distribution at the Electrochemical Interface

Yvonne Gründer and Christopher A. Lucas

*Oliver Lodge Laboratory, Department of Physics, University of Liverpool, Liverpool, L69 7ZE, UK*

## CONTENTS

## *1. Experimental*

For recording the energy dependent scans a Vortec x-ray detector was used. The channels of the detector were calibrated to the specific energy by recording the scattered intensity at energies 400 eV below and 400 eV above the Br edge from the Au sample in 0.1 M $HClO_4$+ 10 mM KBr electrolyte, using the Au fluorescence lines (Figure S1). For each x-ray edge recorded (Cu K, Br K, Au $L_{III}$) both a fluorescence window and an elastic window were set. The region of the elastic window for the Br and Cu K edge are shown by the grey shaded area in Figure S1. In addition the fluorescence window was set from the lowest channel of the detector to the lower limit of the respective window.

Each energy scan was recorded at a fixed position in reciprocal space. Two background scans were recorded by offsetting the θ angle on either side of the peak measured in a rocking scan. The rocking scan was recorded to determine the adequate offset to either side for the signal to be in the background.

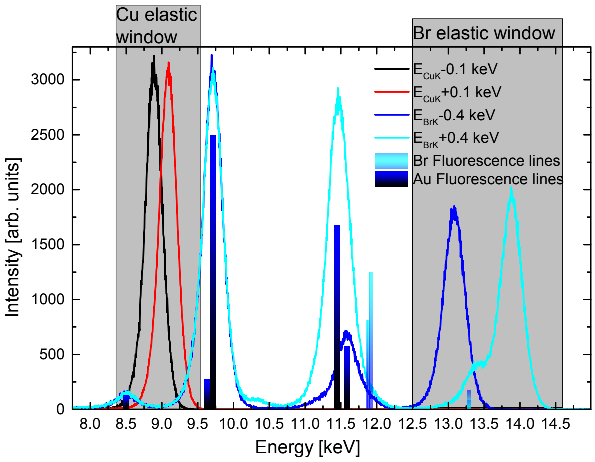

**Figure S1.** The energy resolved signal at a specific point in reciprocal space**.**

Due to the relatively small scattering intensity obtained in the measurements, each energy and background scan was repeated at least once to allow for averaging. The scans were repeated until sufficiently precise counting statistics were acquired.

For the Cu K-edge the spectra were corrected for self-absorption as there is significant fluorescence from the bulk Cu crystal. This was not necessary for the Br-edge data.

The energy resolution of the monochromator on BM28 is 0.7 eV. This was taken into account when modelling the data by convoluting the calculated intensity measured in the the energy scan with a Gaussian function of 0.7 eV full width half maximum (FWHM).

## *2. Supplementary Data:*

### *(a) The L dependence of the resonant signal*

In addition to the data recorded at low L, the intensity on the (1, 1, L) CTR was recorded at L=0.6 and 0.8 while scanning through the Cu-K-edge for the Cu(001)-c(2x2)-Cl superstructure. The data is shown in Figure S2. For L=0.6 and L=0.8 the shift in the edge observed is smaller with ΔE=3.0 ± 0.5 eV and ΔE=2.0 ± 0.5 eV, respectively, compared to ΔE=5.5±0.5 eV at L=0.2. Note that the positions at higher L are not only further away from the surface sensitive anti-Bragg position but that also the angle between the x-ray polarization and the surface normal increases at higher L (from 7° at L=0.2 to 20° for L=0.6 and 28° for L=0.8) due to the fact that the diffractometer was operating in a four-circle geometry mode.

The same positions (along (1, 1, L)) were probed for the Cu(001)-c(2x2)-Br structure (Figure S2) and the data measured at L=0.2 (dark blue curve) gives a shift in the edge position by ΔE=2.0 ± 0.5 eV. Due to the relative scattering strength of the Cu and Br atoms, the decrease in the Cu scattering factor leads to an increase in the intensity at (1, 1, 0.2) at the Cu K edge energy.

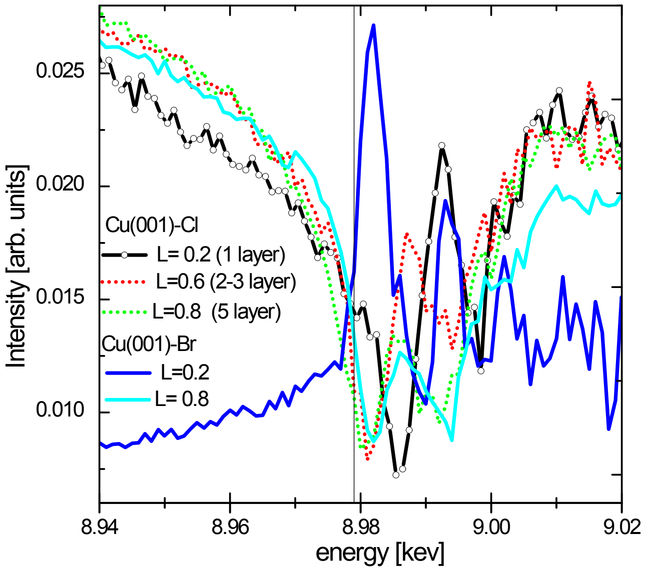

**Figure S2.** The energy scans at different L positions measured on the (1, 1, L) CTR for the

Br and Cl covered Cu(001) surface.

### *(b) Cu(001)-Br: horizontal and vertical geometry*

In addition to the data for the Cl-c(2x2)-Cu(001) structure reported in the manuscript, similar measurements were made for the Br-c(2x2)-Cu(001) structure and are shown here.

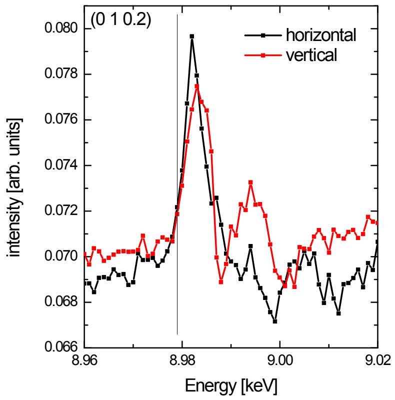

**Figure S3.** The energy scans measured on the c(2x2) superstructure rod at (0, 1, 0.2) for the Br-covered Cu(001) surface obtained in both vertical and horizontal scattering geometries.

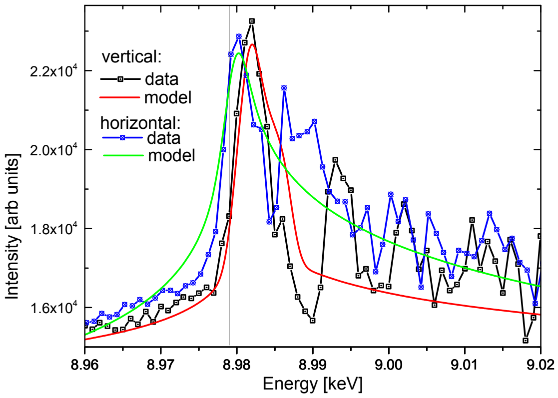

**Figure S4.** The energy scans measured at the (1, 1, 0.2) CTR position for the Br-covered Cu(001) surface in both vertical geometry (x-ray polarization perpendicular to the surface) and horizontal geometry (x-ray polarization in the surface plane). The fits to the data are shown by the solid lines and give a shift of ΔE=2.5 ± 0.5 eV (vertical) and ΔE=0 (horizontal).

### *(c) The Br c(√2 x 2√2)R45° structure on Au(001) probed at the Au $L_{III}$-edge*

For comparison to halide adsorption on Cu(001), resonant surface x-ray diffraction data for bromide adsorption on Au(001) were also recorded. Bromide forms a c(√2 x 2√2)R45°superstructure on Au(001) in a potential range between 0 and 0.4 V vs Ag/AgCl in

10 mM KBr + 0.1 M $HClO_4$. Resonant surface x-ray diffraction data were recorded at the surface sensitive 'anti-Bragg' position of the crystal truncation rod, (1, 1, 0.2), in both the vertical and horizontal scattering geometries at a potential of 0.3 V by scanning the x-ray energy through the Au $L_{III}$-edge (Figure S5). No shift in the x-ray edge position (as compared to Br or Cl on Cu(001) ) in either scattering geometry can be observed.

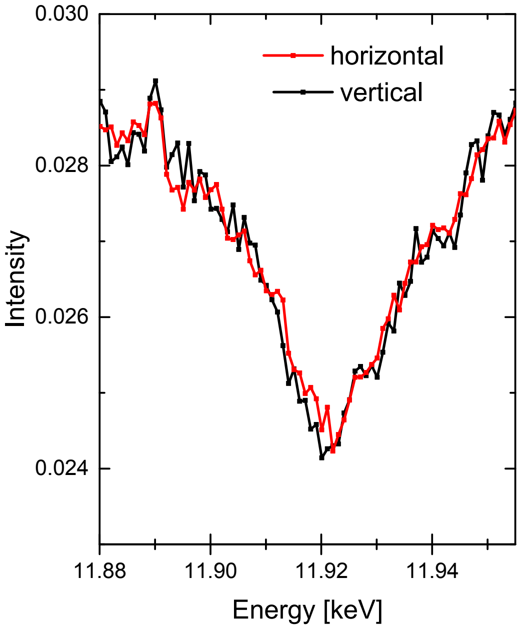

**Figure S5.** The energy scans at the (1, 1, 0.2) CTR position for the Br c(√2 x 2√2)R45°superstructure on Au(001) are shown for the two polarization geometries.

### 3. *Calculation of the edge shift observed*

The scattering of x-rays by an atom is described by the atomic form factor f(Q,E):

$f(\mathbf{Q},E)= f_0(\mathbf{Q})+f'(E)+i f''(E)$, where **Q** is the scattering vector describing the position in reciprocal space and E is the energy of the x-rays. The energy dependence of the atomic form factor comes from the real and imaginary parts, f' and f'' respectively, of the dispersion corrections.

In a non-resonant diffraction measurement the energy of the x-rays and consequently f' and f'' are approximately constant.

The intensity distribution in reciprocal space I(**Q**,E) is the square of the of the total form factor F(**Q**,E). The scattering of x-rays by an ensemble of atoms (e.g. molecule, crystal, surface) can thus be described as: $I(Q,E)=|F(Q,E)|^2=|\sum_j f_j(Q,E)e^{-iQx}|^2$, where **x** is the vector describing the position of the atom in real space.

The atomic positions of all the structures investigated by resonant surface x-ray diffraction have been previously found through surface x-ray diffraction experiments (with fixed x-ray energy E). [1, 2, 3]

The energy dependent contributions f' and f'' to the scattering factors were estimated by using the 'Brennan and Cowan' data from the Dispano software available through the LMPG suite (http://www.ccp14.ac.uk/tutorial/lmgp/) from the Laboratoire des Materiaux et du Génie Physique de l'Ecole Supérieure de Physique de Grenoble.

To reproduce the measured data, the positions of the Cu K-edge for the different atoms close to the interface, specifically the buckled subsurface Cu atoms for measurements at the superstructure position (see Figure S6), and the Cu atoms in the 1st atomic layer for the measurements at the surface sensitive Anti-Bragg positions, were allowed to vary. The relative shift of the edge position was the only free parameter in the calculated fits to the data presented in this manuscript.

## *4. Cu(001)-c(2x2)-halide structure*

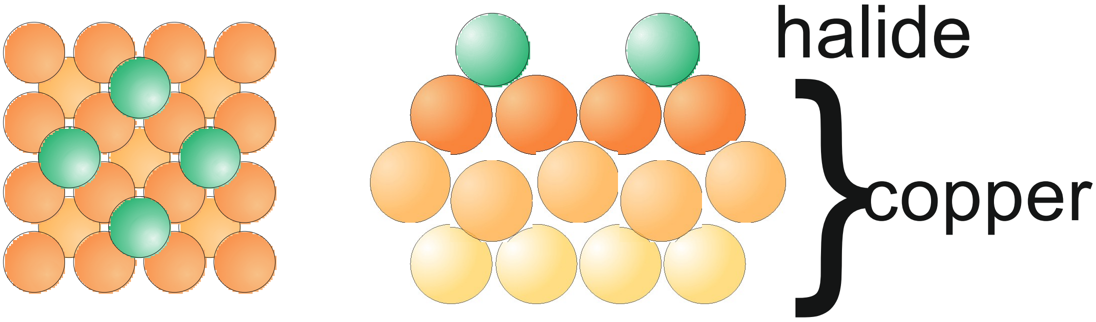

**Figure S6.** Schematic model of the Br/Cl-c(2x2) structure on Cu(001) indicating the sub-surface buckling.

## *5. References*

1. Gründer Y, Kaminski D, Golks F, Krug K, Stettner J, Magnussen OM*, et al.* Reversal of chloride-induced Cu(001) subsurface buckling in the electrochemical environment: An in situ surface x-ray diffraction and density functional theory study. *Phys Rev B Condens Matter Mater Phys* 2010, **81**(17).

2. Gründer Y, Thompson P, Brownrigg A, Darlington M, Lucas CA. Probing the halide-metal interaction by monolayer metal deposition at the electrochemical interface. *Journal of Physical Chemistry C* 2012, **116**(10)**:** 6283-6288.

3. Saracino M, Broekmann P, Gentz K, Becker M, Keller H, Janetzko F*, et al.* Surface relaxation phenomena at electrified interfaces: Revealing adsorbate, potential, and solvent effects by combined x-ray diffraction, STM, and DFT studies. *Physical Review B* 2009, **79:** 115448-115448-115411.